

ABD-Net: Attentive but Diverse Person Re-Identification

Tianlong Chen¹, Shaojin Ding^{1*}, Jingyi Xie^{2*}, Ye Yuan¹, Wuyang Chen¹
 Yang Yang³, Zhou Ren⁴, Zhangyang Wang^{1†}

¹Texas A&M University, ²University of Science and Technology of China

³Walmart Technology, ⁴Wormpex AI Research

{wiwp619,atlaswang}@tamu.edu

Abstract

Attention mechanism has been shown to be effective for person re-identification (Re-ID). However, the learned attentive feature embeddings which are often not naturally diverse nor uncorrelated, will compromise the retrieval performance based on the Euclidean distance. We advocate that enforcing diversity could greatly complement the power of attention. To this end, we propose an Attentive but Diverse Network (ABD-Net), which seamlessly integrates attention modules and diversity regularization throughout the entire network, to learn features that are representative, robust, and more discriminative. Specifically, we introduce a pair of complementary attention modules, focusing on channel aggregation and position awareness, respectively. Furthermore, a new efficient form of orthogonality constraint is derived to enforce orthogonality on both hidden activations and weights. Through careful ablation studies, we verify that the proposed attentive and diverse terms each contributes to the performance gains of ABD-Net. On three popular benchmarks, ABD-Net consistently outperforms existing state-of-the-art methods.

1. Introduction

Person Re-Identification (Re-ID) aims to associate individual identities across time, within a single camera or from cameras at different locations. It embraces many high-impact applications in intelligent video surveillance. Given a query image and a large set of gallery images, person Re-ID firstly represents each image with a *feature embedding*, and then ranks the gallery images in terms of feature embedding similarities to the query. Despite the exciting improvements achieved in recent years, person Re-ID remains to be extremely challenging in practical unconstrained scenarios. Common challenges arise from body misalignment, occlusion, backgrounds, view point changes, pose variations and



Figure 1. Visualization of attention maps. (i) Original images; (ii) Attentive feature maps; (iii) Attentive but diverse feature maps. Diversity can be observed to make attention “broader” in general, and to correct some mistaken over-emphasis (such as clothes textures) by attention. (L: large values; S: small values)

noisy labels, among many others [1].

A great deal of efforts have been devoted to addressing those various challenges. Among them, incorporating body part information [2, 3, 4, 5, 6] has empirically proven to effectively improve the robustness of the features against body misalignment, incomplete parts and occlusions. Partially motivated by so, attention mechanism [7] was introduced to enforce the features to mainly capture the person body (or certain body parts) appearances. Since then, the attention-based deep models [8, 9, 10, 11, 12] have seen much performance boost for person Re-ID.

On a separate note, the feature embeddings will be used to compute similarities, typically based on Euclidean distance, to return the closest matches. Sun et al. [13] pointed out that correlations among feature embeddings would significantly compromise the matching performance. That is, however, not naturally guaranteed in attention-based models. In fact, our observation is that those attention-based models are potentially more prone to causing higher feature correlations, because intuitively, the attention mechanism tends to have features focus on a more compact subspace (such as foreground instead of the full image, see Fig.1 for examples).

In view of the above, we argue that a more desirable fea-

*Equal Contribution.

†Zhangyang Wang is the corresponding author.

ture embedding for person Re-ID should be both **attentive** and **diverse**: the former aims to correct misalignment, to eliminate background perturbation, and to focus on discriminative local parts of body appearances; the latter aims to encourage lower correlation between features and therefore better matching, and potentially increase the representation capacity too. We thus propose an Attentive but Diverse Network (**ABD-Net**) for the task of Person Re-ID, that seamlessly integrates attention modules and diversity regularization and enforces them throughout the entire network. The main contributions of ABD-Net are highlighted as below:

- We incorporate a compound attention mechanism into ABD-Net, consisting of two parts: Channel Attention Module (CAM) and Position Attention Module (PAM). CAM facilitates channel-wise, feature-level information aggregation, while PAM captures the spatial awareness of body and part positions. They are shown to be complementary and altogether benefit Re-ID.
- We introduce a novel regularization term, called spectral value difference orthogonality (SVDO), that directly constrains the conditional number of the weight’s Gram matrix. Efficiently implemented, SVDO is applied to both weight and activation, and is shown to successfully improve feature embedding diversity by reducing their correlations.
- We perform extensive experiments on Market-1501 [14], DukeMTMC-Re-ID [15], and MSMT17 [1]. ABD-Net significantly outperforms the existing methods, and achieves new state-of-the-art on all three popular benchmarks. We also verify that the proposed attentive and diverse terms perform as expected, and each contributes to a part of the performance gains, through carefully-designed ablation studies and visualizations.

We will open-source our codes and pre-trained models upon the paper acceptance.

2. Related Work

2.1. Person Re-identification: Brief Overview

Person Re-ID has two key steps: obtaining a feature embedding and performing matching under some distance metric. For the former, both handcrafted features [16, 17, 18, 19] and learned features [20, 21, 4, 22, 23] were explored. For the latter, various efforts [24, 25, 16] were also adopted. In recent years, the prevailing success of convolutional neural networks (CNNs) in computer vision has made person Re-ID no exception. Due to the problem-specific challenges such as occlusion/misalignment, incomplete body parts, as well as backgrounds/view point changes, naively applying CNN backbones to feature extraction may not yield ideal performance. To enhance the

feature robustness, both global features extracted from the entire image and local features extracted from body parts need to be considered. Many part-based methods have achieved superior performance [2, 3, 26, 27, 28, 4, 5, 29, 6, 30, 31, 8, 32]. We refer readers to [33] for a more comprehensive literature review.

2.2. Attention Mechanisms in Person Re-ID

Several studies proposed to integrate attention mechanism into deep models to address the misalignment issue in person Re-ID. Zhao et al. [8] proposed a part-aligned representation based on a part map detector for each predefined body part. Yao et al. [9] proposed a Part Loss Networks which defined a loss for each average pooled body part and jointly optimized the summation losses. Si et al. [10] proposed a dual attention matching network based on an inter-class and an intra-class attention module to capture the context information of video sequences for person Re-ID. Li et al. [12] proposed a multi-task learning deep model that learns hard region-level and soft pixel-level attention jointly to produce more discriminative feature representations. Xu et al. [11] used pose information to learn attention masks for rigid and non-rigid parts, and then combined the global and part features as the final feature embedding.

Our proposed attention mechanism differs from previous methods in several aspects. First, previous methods [8, 9, 11] only use attention mechanism to extract part-based spatial patterns from person images, usually focused at foregrounds. In contrast, ABD-Net combines spatial and channel attentions; in addition, our added diversity constraint will avoid the attentive features to be correlated and redundant. Second, our attention masks are directly learned from the data and context, without relying on part region proposals nor pose estimation [8, 9, 11]. Besides, our two attention modules are embedded within a single backbone, which differs from and is thus lighter than the multi-task learning model proposed in [11, 12].

2.3. Diversity via Orthogonality

Orthogonality has been widely explored in deep learning to encourage the learning of informative and diverse features. In CNNs, several studies [34, 35, 36, 37] perform regularization using “hard orthogonality constraints”, which typically depend on singular value decomposition (SVD) to strictly constrain their solutions on a Stiefel manifold. A similar idea was first exploited by [13] for person Re-ID, where the authors performed SVD on the weight matrix of the last layer, in an effort to reduce feature correlations. Despite their effectiveness, SVD-based hard orthogonality constraints are computationally expensive, and sometimes overly restricted. Recent studies also investigated “softer” orthogonality regularizations by enforcing the Gram matrix of each weight matrix to be close to identity under Frobe-

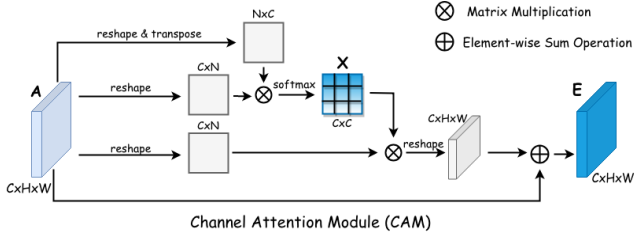


Figure 2. Channel Attention Module (CAM)

nious norm [38] or spectral norm [39]. We propose a novel spectral value difference orthogonality (SVDO) regularization that directly constrains the conditional number of the Gram matrix. Also differently from [13, 38] that apply orthogonality only to CNN weights, we enforce the new regularization on both hidden features and weights.

3. Attentive but Diverse Network

In this section, we first introduce the two attention modules, followed by the new diversity (orthogonality) regularization. We then wrap them up and describe the overall architecture of ABD-Net.

3.1. Attention: Channel-Wise and Position-Wise

The goal of attention for Re-ID is to focus on person-related features while eliminating irrelevant backgrounds. Inspired by the successful idea in segmentation [40], we integrate two complementary attention mechanisms: Channel Attention Module (**CAM**) and Positional Attention Module (**PAM**), throughout the full network. The full configurations for CAM and PAM can be found in the supplementary.

3.1.1 Channel Attention Module

In a trained discriminative CNN, its high-level convolutional channels are regarded as semantic-related and often category-specific. In the person Re-ID case, we hypothesize that some channels might share similar semantic contexts (such as foreground person, occlusions, or background) and are more correlated with each other. CAM is designed to group and aggregate those semantically similar *channels*.

The full structure of CAM is illustrated in Fig.2. Given the input feature maps $\mathbf{A} \in \mathbb{R}^{C \times H \times W}$, where C is the channel number and $H \times W$ the feature map size, we compute the channel affinity matrix $\mathbf{X} \in \mathbb{R}^{C \times C}$, as shown below:

$$x_{ij} = \frac{\exp(A_i \cdot A_j)}{\sum_{j=1}^C \exp(A_i \cdot A_j)}, \quad i, j \in \{1, \dots, C\} \quad (1)$$

where C is the total number of channels, and x_{ij} represents the impact of channel i on channel j . The final output feature map \mathbf{E} is calculated by the equation (2):

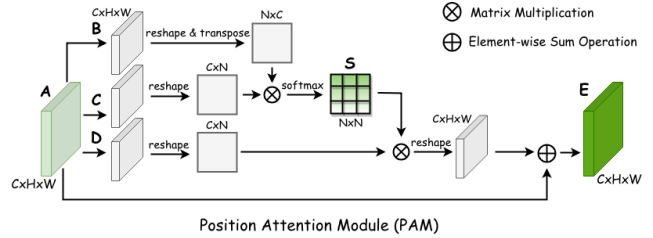


Figure 3. Position Attention Module (PAM)

$$E_i = \gamma \sum_{j=1}^C (x_{ij} A_j) + A_i, \quad i \in \{1, \dots, C\} \quad (2)$$

γ is a hyperparameter to adjust the influence of CAM.

3.1.2 Position Attention Module

The detailed structure of the Position Attention Module (PAM) is illustrated in Fig.3. It is designed to capture and aggregate those semantically related *pixels*. The input feature maps $\mathbf{A} \in \mathbb{R}^{C \times H \times W}$ are first fed into convolution layers with batch normalization and ReLU activation to produce feature maps $\mathbf{B}, \mathbf{C}, \mathbf{D} \in \mathbb{R}^{C \times H \times W}$. Then we compute the pixel affinity matrix $\mathbf{S} \in \mathbb{R}^{N \times N}$, where $N = H \times W$. Note that the dimension between S and X has **difference**, since the former computes correlations between the total N pixels rather than C channels. We generate the final output feature map \mathbf{E} with similar calculation as CAM did in section 3.1.1.

3.2. Diversity: Orthogonality Regularization

Following [13, 39], we enforce diversity via orthogonality, and derive a new orthogonality regularizer term. It can be applied to both hidden features and weights, of both fully-connected and convolutional layers. Orthogonality regularizer on feature space (short for **O.F.** hereinafter) is to enforce informative features that can benefit matching. The orthogonal regularizer on weight (**O.W.**) encourages filter diversity [39] and enhances the learning capacity.

Next, we derive the new orthogonality form on features in details, while the weight orthogonality can be derived similarly*. For feature maps $\mathbf{M} \in \mathbb{R}^{C \times H \times W}$, where C, H, W are channel number, feature map height and feature map width, respectively, we will first reshape \mathbf{M} into a matrix form $\mathbf{F} \in \mathbb{R}^{m' \times n'}$, with $m' = C$ and $n' = H \times W$.

Many orthogonality methods [34, 35, 36, 37], including the prior work in Re-ID [13], fall in the category of

For a convolutional layer $\mathbf{W}_c \in \mathbb{R}^{S \times H \times C \times M}$, where S, H, C, M are filter width, filter height, input channel number and output channel number, respectively, we follow the convention of [38, 39] to reshape \mathbf{W}_c into a matrix form $\mathbf{F}^ \in \mathbb{R}^{m^* \times n^*}$, where $m^* = S \times H \times C$ and $n^* = M$.

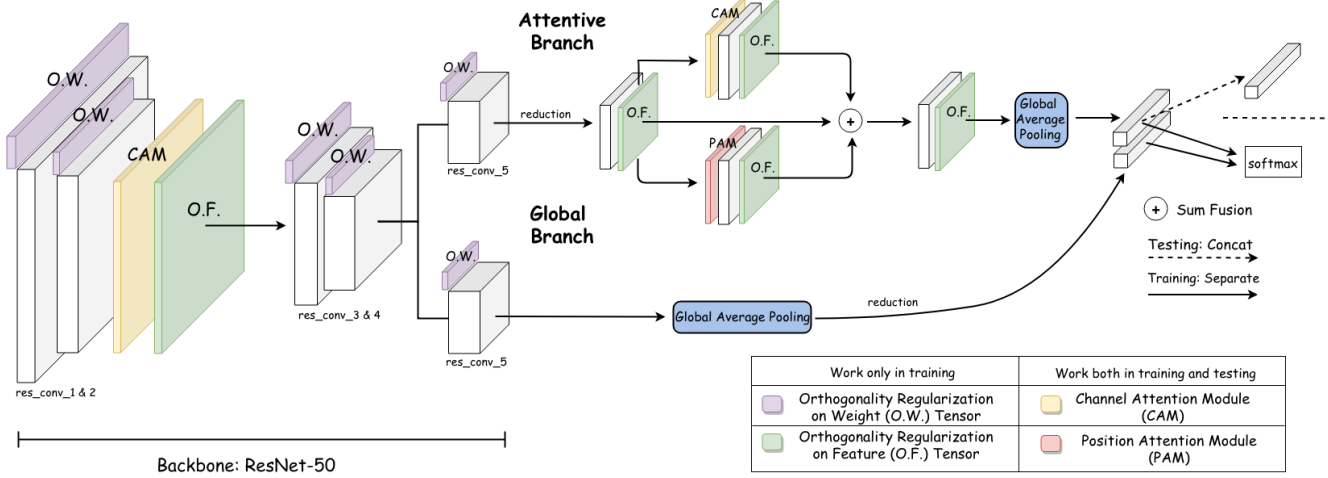


Figure 4. Architecture of ABD-Net: O.W. is applied on all ResNet layers. O.F. is applied after CAM on res_conv_2 and after res_conv_5 in the Attentive Branch. 1 The feature vectors from both attentive and global branches are concatenated as the final feature embedding.

enforcing ‘‘hard orthogonality constraints’’ that have to repeat SVD during training. The cost of SVD on high-dimensional matrices is expensive even in GPUs, which is why we choose to go for softer orthogonality regularizers. Previously, most such regularizers [38, 39, 41] restrict the Gram matrix of \mathbf{F} to be close to identity under the Frobenius norm. It enforces approximate orthogonality among filters or weight columns, leading to smaller correlations among learned features and implicitly reducing the filter redundancy. Such regularizers are also differentiable and require no SVD, thus being computationally cheaper than ‘‘hard constraints’’. However, for an overcomplete \mathbf{F} , the gram matrix cannot be close to identity because of rank deficiency, making the existing soft regularizers biased. More detailed discussions can be found in [38, 39].

Alternatively, we propose to directly enforce the orthogonality via regularizing the conditional number of \mathbf{FF}^T :

$$\beta \|k(\mathbf{F}) - 1\|_2^2, \quad (3)$$

where β is the coefficient and $k(\mathbf{F})$ denotes the condition number of \mathbf{F} , defined as the ratio between maximum and minimum singular values of \mathbf{F} . Naively solving $k(\mathbf{F})$ will take one full SVD. To make it computationally more tractable, we first convert (3) into a spectral value difference orthogonality (SVDO)[†] regularization:

$$\beta \|\lambda_1(\mathbf{FF}^T) - \lambda_2(\mathbf{FF}^T)\|_2^2, \quad (4)$$

where $\lambda_1(\mathbf{FF}^T)$ and $\lambda_2(\mathbf{FF}^T)$ denote the largest and smallest eigenvalues of \mathbf{FF}^T , respectively.

[†]The reason why we choose to penalize the difference between $\lambda_1(\mathbf{FF}^T)$ and $\lambda_2(\mathbf{FF}^T)$ rather than the ratio of them is to avoid numerical instability caused by dividing a very small $\lambda_2(\mathbf{FF}^T)$, which we find common in our experiments.

We next refer to auto differentiation to compute the gradient of SVDO w.r.t. \mathbf{F} for simplicity. However, computing the objective value of equation (4) still invokes the expensive eigenvalue decomposition (EVD). To bypass EVD, we approximate the computation of eigenvalues with the power iteration method. We first start with a random initialized v , and then iteratively perform the following routine (2 times in this paper):

$$u \leftarrow \mathbf{X}v, v \leftarrow \mathbf{X}u, \lambda(\mathbf{X}) \leftarrow \frac{\|v\|}{\|u\|}. \quad (5)$$

where \mathbf{X} in equation (5) is \mathbf{FF}^T for computing $\lambda_1(\mathbf{FF}^T)$, and is $\mathbf{FF}^T - \lambda_1 \mathbf{I}$ for $\lambda_2(\mathbf{FF}^T)$. With such approximation been implemented, SVDO becomes practically very fast in our implementation.

3.3. The Network Architecture Overview

The architecture of the proposed ABD-Net is shown in Fig.4. ABD-Net is compatible with most common feature extraction backbones, such as ResNet [42], InceptionNet [43], and Densenet [44]. Unless otherwise specified, we use ResNet-50 as the default backbone network due to its popularity in Re-ID [45, 46, 47, 48, 49, 11, 50, 51].

We add a CAM and O.F. on the outputs of res_conv_2 block. The regularized feature map is used as the input of res_conv_3. Next, after the res_conv_4 block, the network splits into a *global branch* and an *attentive branch* in parallel. We apply O.W. on all conv layers in our ResNet-50 backbone, *i.e.*, from res_conv_1 to res_conv_4 and the two res_conv_5 in both branches. The outputs of two branches are concatenated as the final feature embedding.

In the *attentive branch*, we use the same res_conv_5 layer as that in ResNet-50. We then feed the output feature map

into a reduction layer[‡] with O.F. applied, which yields a smaller feature map \mathbf{T}_a . Afterward, we feed \mathbf{T}_a into a CAM and a PAM simultaneously, both with O.F. constraints. The outputs from both attentive modules are concatenated with the input \mathbf{T}_a , and all together go through a global average pooling layer, ending up with a k_a -dimension feature vector.

In the *global branch*, after `res.conv_5`[§], the feature map \mathbf{T}_g is fed into a global average-pooling layer followed by a reduction layer, leading to a k_g -dimension feature vector. The global branch intends to preserve global context information in addition to the attentive branch features.

Eventually, the ABD-Net is trained under the loss function L consisting of cross entropy loss, hard mining triplet loss, orthogonal constraints on feature (O.F.) and on weights (O.W.) penalty terms (each weighted by a hyper-parameter):

$$L = L_{xent} + \beta_{tr} L_{triplet} + \beta_{O.F.} L_{O.F.} + \beta_{O.W.} L_{O.W.} \quad (6)$$

where $L_{O.F.}$ and $L_{O.W.}$ stand for the SVDO penalty term applied to the hiden features and weights, respectively.

4. Experiments

To evaluate ABD-Net, we conducted experiments on three large-scale datasets: Market-1501 [14], DukeMTMC-Re-ID [15] and MSMT17 [1]. First, we report an ablation study (mainly on Market-1501 and DukeMTMC-Re-ID) to validate the effectiveness of each component. Second, we compare the performance of ABD-Net against existing state-of-the-art methods on all three datasets. Finally, we provide more visualizations and analysis to illustrate how ABD-Net has achieved its effectiveness.

4.1. Datasets

Market-1501 [14] comprises 32,668 labeled images of 1,501 identities captured by six cameras. Following [14], 12,936 images of 751 identities are used for training, while the rest are used for testing. Among the testing data, the test probe set is ficed with 3,368 images of 750 identities. The test gallery set also includes 2,793 additional distractors.

DukeMTMC-Re-ID [15] contains 36,411 images of 1,812 identities. These images are captured by eight cameras, among which, 1,404 identities appear in more than two cameras and 408 identities (distractors) appear in only one camera. The 1,404 identities are randomly divided, with 702 identities for training and the others for testing. In the testing set, one query image for each ID per camera is chosen for the probe set, while all remaining images including distractors are in the gallery.

[‡]A reduction layer consists of a linear layer, batch normalization, ReLU, and dropout. See: <https://github.com/KaiyangZhou/deep-person-reid>

[§]For both two `res.conv_5` in two branches, we removed the down-sampling layer, in order for a larger feature map

MSMT17 [1] is the current largest publicly-available person Re-ID dataset. It has 126,441 images of 4,101 identities captured by a 15-camera network (12 outdoor, 3 indoor). We follow the training-testing split of [1]. The video is collected with different weather conditions at three-time slots (morning, noon, afternoon). All annotations, including camera IDs, weathers and time slots, are available. MSMT17 is **significantly more challenging** than the other two, due to its massive scale, more complex and dynamic scenes. Additionally, the amount of methods that report on this dataset is limited since it is recently released.

4.2. Implementation Details and Evaluation

Implementation Details During training, the input images are re-sized to 384×128 and then augmented by random horizontal flip, normalization, and random erasing [52]. The testing images are re-sized to 384×128 and augmented only with normalization. In our experiments, the sizes of \mathbf{T}_a and \mathbf{T}_g are $1024 \times 24 \times 8$, and $2048 \times 24 \times 8$, respectively. We set $k_a = k_g = 1024$, leading to a 2048-dimensional feature embedding for matching.

With the ImageNet-pretrained ResNet-50 backbone, we used the two-step transfer learning algorithm [53] to fine-tune the model. First, we freeze the backbone weights and only trained the reduction layers, classifiers and all attention modules for 10 epochs, with only the cross entropy loss and triplet loss applied. Second, all layers are freed for training for another 60 epochs, with the full loss (6) applied. We set $\beta_{tr} = 10^{-1}$, $\beta_{OF} = 10^{-6}$ and $\beta_{OW} = 10^{-3}$, and the margin parameter for triplet loss $\alpha = 1.2$.

Our network is trained using 2 Tesla P100 GPUs with a batch size of 64. Each batch contains 16 identities, with 4 instances per identity. We use the Adam optimizer with the base learning rate initialized to 3×10^{-4} , then decayed to 3×10^{-5} , 3×10^{-6} after 30, 40 epochs, respectively. The training takes about 4 hours on the Market-1501 dataset.

We adopt standard person Re-ID metrics: the top-1 accuracy, and the mean Average Precision (mAP). We consider mAP to be more reliable an indicator for Re-ID performance.

4.3. Ablation Study of ABD-Net

To verify the effects of attention modules and orthogonality regularization in ABD-Net, we evaluate each module in an incremental manner on Market-1501 and DukeMTMC-Re-ID. We choose ResNet-50[¶] with the cross entropy loss (XE) as the baseline. Nine variants are then constructed on top of the baseline^{||}: a) baseline (XE) + O.F.;

[¶]For the fair of ablation study, we use two duplicated branches with the same `res.conv_5` like the structure in ABD-Net as shown in Fig.4. Data augmentation and dropout are applied.

^{||}Note that (1) CAM is used in two places of ABD-Net; (2) ABD-Net adopts O.F. + O.W. + PAM + CAM.

b) baseline (XE) + O.W.; **c)** baseline (XE) + O.F. + O.W.; **d)** baseline + SVD layer (similar to SVD-Net [13]); **e)** baseline (XE) + PAM; **f)** baseline (XE) + CAM; **g)** baseline (XE) + PAM + CAM; **h)** ABD-Net (XE), that sets $\beta_{tr} = 0$ in (6); and **i)** ABD-Net, that uses the full loss (6).

Table 1. Ablation Study of ABD-Module on Market-1501. O.F. and O.W. : Orthogonality Regularization on Features and Weights; PAM and CAM: Position and Channel Attention Modules.

Method	Market-1501		DukeMTMC	
	top1	mAP	top1	mAP
baseline (XE)	91.50	77.40	82.80	66.40
baseline (XE) + O.F.	92.90	82.10	84.90	71.30
baseline (XE) + O.W.	92.50	78.50	83.70	67.40
baseline (XE) + O.F. + O.W.	93.20	82.30	85.30	72.20
baseline + SVD layer	90.80	76.90	79.40	62.50
baseline (XE) + PAM	92.10	78.10	83.80	67.00
baseline (XE) + CAM	91.80	78.00	84.30	67.60
baseline (XE) + PAM + CAM	92.70	78.50	84.40	67.90
ABD-Net (XE)	94.90	85.90	87.30	76.00
ABD-Net	95.60	88.28	88.30	78.20

Table 1 presents the ablation results, from which a number of observations could be drawn with good consistency:

- Using either O.F. or O.W. consistently outperforms the top-1 and mAP of the baseline on both two datasets, and their combination leads to further gains which validates the effectiveness of adding diverse regularization in training ReID models. We also observe our proposed SVDO-based O.W. to empirically perform better than the SVD layer**, potentially due as the former being “softer” and more flexible.
- Using either PAM and CAM improves over the baseline on both datasets too, and combining them improves over either alone, demonstrating the complementary power of two different attention mechanism.
- By combining “attention” and “diverse”, ABD-Net (XE) obtains further boosted performance. For example, on Market-1501, ABD-Net (XE) outperforms the “no attention” counterpart (baseline (XE) + O.F. + O.W.) by a margin of 1.50% (top-1)/3.60 (mAP), and outperforms “no diversity” counterpart (baseline (XE) + O.F. + O.W.) by 2.20% (top-1)/7.40 (mAP). Finally, the proposed full ABD-Net further benefits from adding triplet loss.

4.4. Comparison to State-of-the-art Methods

We compare ABD-Net against the state-of-the-art methods on Market-1501, DukeMTMC-Re-ID and MSMT17, as

**Our results of baseline + SVD layer is better than SVDNet [13, 52], but worse than baseline (XE). A possible reason is that SVD layer is a “hard constraint” so that it contributes little to our backbone.

Table 2. Comparison to state-of-the-art on Market-1501. **Red** denotes our performance, and **Blue** denotes the best performance reported by existing methods: the same hereinafter.

Method	Market-1501	
	top1	mAP
BOW [54] (2015 ICCV)	44.42	20.76
Re-Rank [55] (2017 CVPR)	77.11	63.63
SSM [56] (2017 CVPR)	82.21	68.80
SVDNet(RE) [52] (2017 CVPR)	87.08	71.31
AWTL [57] (2018 CVPR)	84.20	68.03
DSR [58] (2018 CVPR)	83.68	64.25
MLFN [59] (2018 CVPR)	90.00	74.30
Deep CRF [60] (2018 CVPR)	93.50	81.60
Deep KPM [61] (2018 CVPR)	90.10	75.30
HAP2S [62] (2018 ECCV)	84.20	69.76
SGGNN [63] (2018 ECCV)	92.30	82.08
Part-aligned [31] (2018 ECCV)	91.70	79.60
PCB [64] (2018 ECCV)	93.80	81.60
SNL [45] (2018 ACM MM)	88.27	73.43
HDLF [46] (2018 ACM MM)	93.30	79.10
‡ MGN [47] (2018 ACM MM)	95.70	86.90
‡ Local CNN [48] (2018 ACM MM)	95.90	87.40
* MGCAM [49] (2018 CVPR)	83.79	74.33
* AACN [11] (2018 CVPR)	85.90	66.87
* HA-CNN [50] (2018 CVPR)	91.20	75.70
* CA ³ Net [51] (2018 CVPR)	93.20	80.00
* Manes [65] (2018 ECCV)	93.10	82.30
* A ³ M [66] (2018 ACM MM)	86.54	68.97
• SPReID [67] (2018 CVPR)	93.68	83.36
* ◇ DuATM [68] (2018 CVPR)	91.42	76.62
ABD-Net	95.60	88.28

* This also exploits attention mechanisms.

• This is with a **ResNet-152** backbone.

◇ This is with a **DenseNet-121** backbone.

‡ Official codes are not released. We report the numbers in the original paper, which are better than our re-implementation.

shown in Tables 2, 3, and 4, respectively. For fair comparison, no post-processing such as re-ranking [55] or multi-query fusion [54] was used for our methods.

On all datasets, ABD-Net has clearly yielded overall state-of-the-art performance. Specifically, on DukeMTMC-Re-ID, ABD-Net obtains 89.00% top-1 accuracy and 78.59% mAP, which significantly outperforms all existing methods. On MSMT17, ABD-Net presents a clear winner case too. On Market-1501, its top-1 accuracy (95.60%) slightly lags behind Local CNN [48] (95.90%) and MGN [47] (95.70%); yet ABD-Net clearly surpasses all existing methods in terms of mAP (88.28; outperforming the closest competitor [48] by 0.88).

Specifically, we compare ABD-Net with several existing attention-based Re-ID methods (labeled by * in the Tables 2 3). As shown in Table 2 and 3, ABD-Net achieved at least

Table 3. Comparison to state-of-the-art on DukeMTMC.

Method	DukeMTMC-Re-ID	
	top1	mAP
BOW [54] (2015 ICCV)	25.13	12.17
SVDNet [13] (2017 ICCV)	76.70	56.80
SVDNet(RE) [52] (2017 CVPR)	79.31	62.44
FMN [69] (2017 CVPR)	74.51	56.88
PAN [70] (2018 TCSVT)	71.59	51.51
AWTL(2-stream) [57] (2018 CVPR)	79.80	63.40
Deep-person [71] (2018 CVPR)	80.90	64.80
MLFN [59] (2018 CVPR)	81.20	62.80
GP-Re-ID [72] (2018 CVPR)	85.20	72.80
PCB [64] (2018 ECCV)	83.30	69.20
Part-aligned [31] (2018 ECCV)	84.40	69.30
‡ MGN [47] (2018 ACM MM)	88.70	78.40
‡ Local CNN [48] (2018 ACM MM)	82.23	66.04
* AACN [11] (2018 CVPR)	76.84	59.25
* HA-CNN [50] (2018 CVPR)	80.50	63.80
* CA ³ Net [51] (2018 CVPR)	84.60	70.20
* Mancs [65] (2018 ECCV)	84.90	71.80
• SPReID [67] (2018 CVPR)	85.95	73.34
* ◇ DuATM [68] (2018 CVPR)	78.74	62.26
ABD-Net	89.00	78.59

* This also exploits attention mechanisms.

• This is with a **ResNet-152** backbone.

◇ This is with a **DenseNet-121** backbone.

‡ Official codes are not released. We report the numbers in the original paper, which are better than our re-implementation.

Table 4. Comparison to state-of-the-art on MSMT17.

Method	MSMT17		
	top1	top5	mAP
PDC [5] (2017 ICCV)	58.00	73.60	29.70
GLAD [29] (2017 ACM MM)	61.40	76.80	34.00
ABD-Net	82.30	90.60	60.80

2.40% top-1 and 5.98 mAP improvement on Market-1501, compared to the closest attention-based prior work CA³Net [51]. On DukeMTMC, the margins becomes 3.40% top-1 and 6.40 mAP. We also look at the SVDNet [13] and HA-CNN [50] which also proposed to generate more diverse and representative feature embeddings. ABD-Net surpasses both with significant top-1 and mAP advantages. Overall, our observation appears to endorse the superiority of ABD-Net by combining “attentive” and “diverse”.

4.5. Visualizations

Attention Pattern Visualization: We conduct a set of attention visualizations^{††} on the final output feature maps of the baseline (XE), baseline (XE) + PAM + CAM, and

^{††}Grad-CAM visualization method [73]: <https://github.com/utkuozbulak/pytorch-cnn-visualizations>

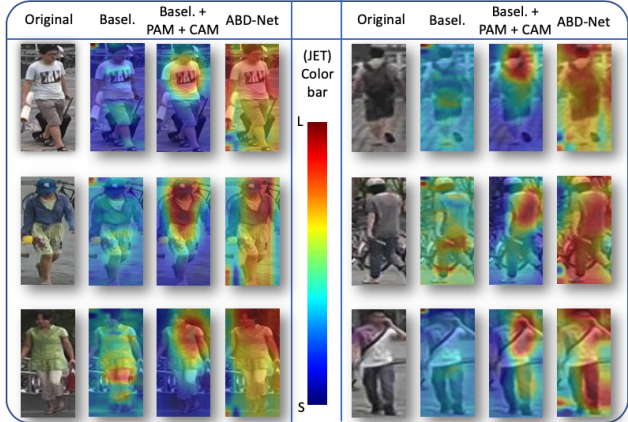


Figure 5. Visualization of attention maps from Baseline, Baseline + PAM + CAM and ABD-Net (XE).

ABD-Net (XE)^{‡‡}, as shown in Fig.5. We notice that the feature maps from the baseline show little attentiveness. PAM + CAM enforce the network to focus more on the person region, but the attention regions can sometimes overly emphasize some local regions (e.g., clothes), implying the risk of over fitting person-irrelevant nuisances. Most channels focus on the similar region may also cause a high correlation in the feature embedding. In contrast, the attention of ABD-Net (XE) can strike a better balance: it focuses on more local parts of the person body while still being able to eliminate the person from backgrounds. The attention patterns now differ more from person to person, and the feature embeddings become more decorrelated and diverse.

Feature De-correlation: We study the correlation matrix between the channel outputs produced by Baseline, Baseline + PAM + CAM and ABD-Net (XE)^{§§}. The feature embedding before the global average pooling is reshaped into $\mathbf{F} \in \mathbb{R}^{C \times N}$, where $N = H \times W$. Then, we compute and visualize the correlation coefficient matrix for \mathbf{F} , denoted as $\mathbf{Corr} \in \mathbb{R}^{C \times C}$ ^{¶¶} in Fig.6. We can observe that, the baseline feature embeddings generally have low correlations. However, after attending PAM + CAM, the feature embedding correlations become much larger, supporting our hypothesis that the attention mechanism tends to encourage more “focused” and thus likely correlated features. Fortunately, with ABD-Net (XE) adding the orthogonality regularization, the feature correlations get greatly suppressed compared to the attention-only case. The feature histogram plots in Fig.7 also certify the same observation. To quantify the comparison, we define $S(\mathbf{Corr})$ as the average of all correlation coefficients in \mathbf{Corr} . For Baseline,

^{‡‡}Here we did not use our best model ABD-Net, since we hope to ensure the fair comparison of the three methods, using the same XE loss.

^{§§}We used the top right testing image in Fig.5 as the example.

^{¶¶}We take the absolute value for correlation coefficients.

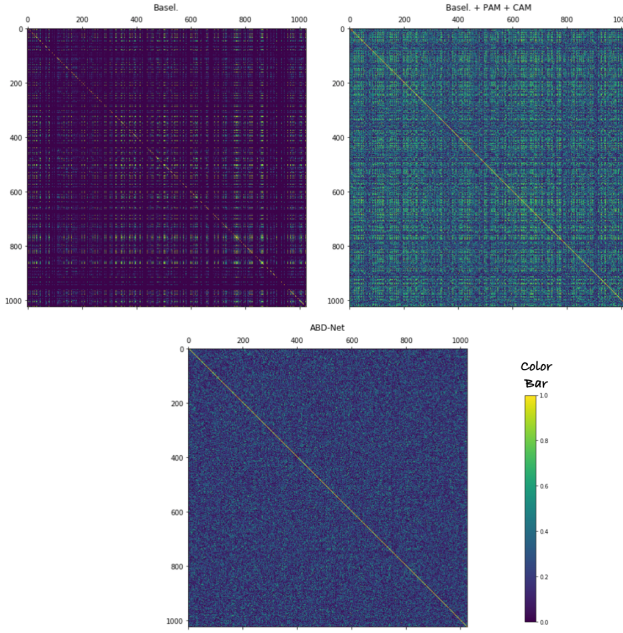


Figure 6. Visualization of correlation matrix between channels from Baseline, Baseline + PAM + CAM and ABD-Net (XE). Brighter color indicates larger correlation.

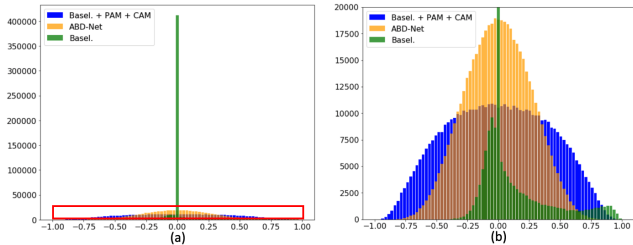


Figure 7. Histogram of correlation from Baseline, Baseline + PAM + CAM and ABD-Net (XE). More skewed distribution indicates more de-correlated feature embeddings. (b) is a zoom-in of the red box area in (a).

Baseline + PAM + CAM, and ABD-Net (XE), $S(\text{Corr}) = 0.05, 0.34$ and 0.21 , respectively.

Features Embedding: Fig.8 shows the t-SNE visualization on feature distributions from Baseline, Baseline + PAM + CAM and ABD-Net (XE) using t-SNE. Compared with Baseline, although attentive features from Baseline + PAM + CAM is a little more distinguishable for the two IDs (94 and 156) in cycle B, it enlarges the intra-class distance of ID 521 in cycle A. Fortunately, in ABD-Net, the features from ID 94 and ID 156 become more discriminative, and the features from ID 521 also lie in a much smaller region.

Re-ID Qualitative Results: Fig.9 shows four Re-ID examples of ABD-Net (XE), Baseline + PAM + CAM and Baseline on Market-1501. Fig.9 (a), (b) and (c) indicate that ABD-Net succeeds in finding more true positives than

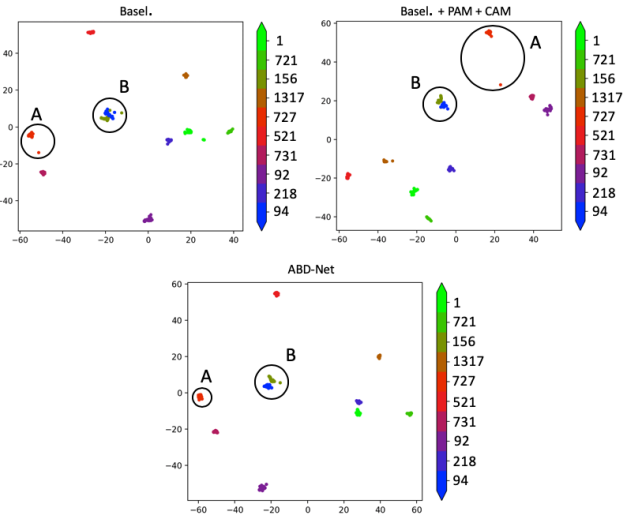


Figure 8. t-SNE visualization of feature distributions, from Baseline, Baseline + PAM + CAM and ABD-Net (XE). Ten identities are randomly selected from the Market-1501 and their IDs are listed on the right side of graphs. Circle A contains the features from ID 521; Circle B contains the features from ID 94 and ID 156.



Figure 9. Four Re-ID examples of ABD-Net (XE), Baseline + PAM + CAM and Baseline on Market-1501. Left: query image. Right: i): top-5 results of ABD-Net (XE). ii): top-5 results of Baseline + PAM + CAM. iii): top-5 results of Baseline. Images in red boxes are negative results.

Baseline + PAM + CAM model, even though the person in the images is under significant view changes and appearance variations. Fig.9 (d) has a failure case of ABD-Net, where the person with similar legs, cloth, hair, and bag are presented.

5. Conclusion

This paper proposed a novel Attentive but Diverse Network (ABD-Net), to learn more representative, robust, discriminative feature embeddings for person Re-ID. Through extensive experiments, ABD-Net demonstrated state-of-the-art performance, where the ablations and visualization show each added component substantially contribute to its final performance. In future, we will explore the use of other attention mechanism with diversity constraints in ABD-Net and generalize ABD-Net to other computer vision tasks.

References

- [1] Longhui Wei, Shiliang Zhang, Wen Gao, and Qi Tian. Person transfer gan to bridge domain gap for person re-identification. In *The IEEE Conference on Computer Vision and Pattern Recognition (CVPR)*, June 2018. [1](#), [2](#), [5](#)
- [2] Douglas Gray and Hai Tao. Viewpoint invariant pedestrian recognition with an ensemble of localized features. In *European conference on computer vision*, pages 262–275. Springer, 2008. [1](#), [2](#)
- [3] Bryan James Prosser, Wei-Shi Zheng, Shaogang Gong, Tao Xiang, and Q Mary. Person re-identification by support vector ranking. In *BMVC*, volume 2, page 6, 2010. [1](#), [2](#)
- [4] De Cheng, Yihong Gong, Sanping Zhou, Jinjun Wang, and Nanning Zheng. Person re-identification by multi-channel parts-based cnn with improved triplet loss function. In *Proceedings of the IEEE Conference on Computer Vision and Pattern Recognition*, pages 1335–1344, 2016. [1](#), [2](#)
- [5] Chi Su, Jianing Li, Shiliang Zhang, Junliang Xing, Wen Gao, and Qi Tian. Pose-driven deep convolutional model for person re-identification. In *Computer Vision (ICCV), 2017 IEEE International Conference on*, pages 3980–3989. IEEE, 2017. [1](#), [2](#), [7](#)
- [6] Liang Zheng, Yujia Huang, Huchuan Lu, and Yi Yang. Pose invariant embedding for deep person re-identification. *arXiv preprint arXiv:1701.07732*, 2017. [1](#), [2](#)
- [7] Ashish Vaswani, Noam Shazeer, Niki Parmar, Jakob Uszkoreit, Llion Jones, Aidan N Gomez, Łukasz Kaiser, and Illia Polosukhin. Attention is all you need. In *Advances in Neural Information Processing Systems*, pages 5998–6008, 2017. [1](#)
- [8] Liming Zhao, Xi Li, Yueteng Zhuang, and Jingdong Wang. Deeply-learned part-aligned representations for person re-identification. In *ICCV*, pages 3239–3248, 2017. [1](#), [2](#)
- [9] Hantao Yao, Shiliang Zhang, Yongdong Zhang, Jintao Li, and Qi Tian. Deep representation learning with part loss for person re-identification. *arXiv preprint arXiv:1707.00798*, 2017. [1](#), [2](#)
- [10] Jianlou Si, Honggang Zhang, Chun-Guang Li, Jason Kuen, Xiangfei Kong, Alex C Kot, and Gang Wang. Dual attention matching network for context-aware feature sequence based person re-identification. *arXiv preprint arXiv:1803.09937*, 2018. [1](#), [2](#)
- [11] Jing Xu, Rui Zhao, Feng Zhu, Huaming Wang, and Wanli Ouyang. Attention-aware compositional network for person re-identification. *arXiv preprint arXiv:1805.03344*, 2018. [1](#), [2](#), [4](#), [6](#), [7](#)
- [12] Wei Li, Xiatian Zhu, and Shaogang Gong. Harmonious attention network for person re-identification. In *CVPR*, volume 1, page 2, 2018. [1](#), [2](#)
- [13] Yifan Sun, Liang Zheng, Weijian Deng, and Shengjin Wang. Svdnet for pedestrian retrieval. In *2017 IEEE International Conference on Computer Vision (ICCV)*, Oct 2017. [1](#), [2](#), [3](#), [6](#), [7](#)
- [14] Liang Zheng, Liyue Shen, Lu Tian, Shengjin Wang, Jingdong Wang, and Qi Tian. Scalable person re-identification: A benchmark. In *The IEEE International Conference on Computer Vision (ICCV)*, December 2015. [2](#), [5](#)
- [15] Ergys Ristani, Francesco Solera, Roger Zou, Rita Cucchiara, and Carlo Tomasi. Performance measures and a data set for multi-target, multi-camera tracking. In *The European Conference on Computer Vision (ECCV)*, September 2016. [2](#), [5](#)
- [16] Sameh Khamis, Cheng-Hao Kuo, Vivek K Singh, Vinay D Shet, and Larry S Davis. Joint learning for attribute-consistent person re-identification. In *European Conference on Computer Vision*, pages 134–146. Springer, 2014. [2](#)
- [17] Martin Koestinger, Martin Hirzer, Paul Wohlhart, Peter M Roth, and Horst Bischof. Large scale metric learning from equivalence constraints. In *Computer Vision and Pattern Recognition (CVPR), 2012 IEEE Conference on*, pages 2288–2295. IEEE, 2012. [2](#)
- [18] Wei Li and Xiaogang Wang. Locally aligned feature transforms across views. In *Proceedings of the IEEE Conference on Computer Vision and Pattern Recognition*, pages 3594–3601, 2013. [2](#)
- [19] Bingpeng Ma, Yu Su, and Frédéric Jurie. Bicov: a novel image representation for person re-identification and face verification. In *British Machine Vision Conference*, pages 11–pages, 2012. [2](#)
- [20] Wei Li, Rui Zhao, Tong Xiao, and Xiaogang Wang. Deep-reid: Deep filter pairing neural network for person re-identification. In *Proceedings of the IEEE Conference on Computer Vision and Pattern Recognition*, pages 152–159, 2014. [2](#)
- [21] Rui Zhao, Wanli Ouyang, and Xiaogang Wang. Learning mid-level filters for person re-identification. In *Proceedings of the IEEE Conference on Computer Vision and Pattern Recognition*, pages 144–151, 2014. [2](#)
- [22] Alexander Hermans, Lucas Beyer, and Bastian Leibe. In defense of the triplet loss for person re-identification. *arXiv preprint arXiv:1703.07737*, 2017. [2](#)
- [23] Wentong Liao, Michael Ying Yang, Ni Zhan, and Bodo Rosenhahn. Triplet-based deep similarity learning for person re-identification. In *Proceedings of the 2017 IEEE International Conference on Computer Vision Workshop (ICCVW)*, pages 385–393, 2017. [2](#)

[24] Kilian Q Weinberger, John Blitzer, and Lawrence K Saul. Distance metric learning for large margin nearest neighbor classification. In *Advances in neural information processing systems*, pages 1473–1480, 2006. 2

[25] Zhen Li, Shiyu Chang, Feng Liang, Thomas S Huang, Lian-giang Cao, and John R Smith. Learning locally-adaptive decision functions for person verification. In *Proceedings of the IEEE Conference on Computer Vision and Pattern Recognition*, pages 3610–3617, 2013. 2

[26] Shengcai Liao, Yang Hu, Xiangyu Zhu, and Stan Z Li. Person re-identification by local maximal occurrence representation and metric learning. In *Proceedings of the IEEE conference on computer vision and pattern recognition*, pages 2197–2206, 2015. 2

[27] Andy J Ma, Pong C Yuen, and Jiawei Li. Domain transfer support vector ranking for person re-identification without target camera label information. In *Proceedings of the IEEE International Conference on Computer Vision*, pages 3567–3574, 2013. 2

[28] Wei-Shi Zheng, Shaogang Gong, and Tao Xiang. Reidentification by relative distance comparison. *IEEE transactions on pattern analysis and machine intelligence*, 35(3):653–668, 2013. 2

[29] Longhui Wei, Shiliang Zhang, Hantao Yao, Wen Gao, and Qi Tian. Glad: global-local-alignment descriptor for pedestrian retrieval. In *Proceedings of the 2017 ACM on Multimedia Conference*, pages 420–428. ACM, 2017. 2, 7

[30] Fuqing Zhu, Xiangwei Kong, Liang Zheng, Haiyan Fu, and Qi Tian. Part-based deep hashing for large-scale person re-identification. *IEEE Transactions on Image Processing*, 26(10):4806–4817, 2017. 2

[31] Yumin Suh, Jingdong Wang, Siyu Tang, Tao Mei, and Kyoung Mu Lee. Part-aligned bilinear representations for person re-identification. *arXiv preprint arXiv:1804.07094*, 2018. 2, 6, 7

[32] Haiyu Zhao, Maoqing Tian, Shuyang Sun, Jing Shao, Junjie Yan, Shuai Yi, Xiaogang Wang, and Xiaou Tang. Spindle net: Person re-identification with human body region guided feature decomposition and fusion. In *Proceedings of the IEEE Conference on Computer Vision and Pattern Recognition*, pages 1077–1085, 2017. 2

[33] Liang Zheng, Yi Yang, and Alexander G Hauptmann. Person re-identification: Past, present and future. *arXiv preprint arXiv:1610.02984*, 2016. 2

[34] Stéfan van der Walt, S. Chris Colbert, and Gaél Varoquaux. The numpy array: a structure for efficient numerical computation. *CoRR*, abs/1102.1523, 2011. 2, 3

[35] Mehrtash Harandi and Basura Fernando. Generalized backpropagation,\'{E} tude de cas: Orthogonality. *arXiv preprint arXiv:1611.05927*, 2016. 2, 3

[36] Mete Ozay and Takayuki Okatani. Optimization on submanifolds of convolution kernels in cnns, 2016. 2, 3

[37] Lei Huang, Xianglong Liu, Bo Lang, Adams Wei Yu, Yongliang Wang, and Bo Li. Orthogonal weight normalization: Solution to optimization over multiple dependent stiefel manifolds in deep neural networks, 2017. 2, 3

[38] Di Xie, Jiang Xiong, and Shiliang Pu. All you need is beyond a good init: Exploring better solution for training extremely deep convolutional neural networks with orthonormality and modulation. *2017 IEEE Conference on Computer Vision and Pattern Recognition (CVPR)*, Jul 2017. 3, 4

[39] Nitin Bansal, Xiaohan Chen, and Zhangyang Wang. Can we gain more from orthogonality regularizations in training deep networks? In *Advances in Neural Information Processing Systems*, pages 4266–4276, 2018. 3, 4

[40] Jun Fu, Jing Liu, Haijie Tian, Zhiwei Fang, and Hanqing Lu. Dual attention network for scene segmentation. *arXiv preprint arXiv:1809.02983*, 2018. 3

[41] Emmanuel Candes and Terence Tao. Decoding by linear programming. *arXiv preprint math/0502327*, 2005. 4

[42] Kaiming He, Xiangyu Zhang, Shaoqing Ren, and Jian Sun. Deep residual learning for image recognition. In *Proceedings of the IEEE conference on computer vision and pattern recognition*, pages 770–778, 2016. 4

[43] Christian Szegedy, Sergey Ioffe, Vincent Vanhoucke, and Alexander A Alemi. Inception-v4, inception-resnet and the impact of residual connections on learning. In *Thirty-First AAAI Conference on Artificial Intelligence*, 2017. 4

[44] Gao Huang, Zhuang Liu, Laurens Van Der Maaten, and Kilian Q Weinberger. Densely connected convolutional networks. In *Proceedings of the IEEE conference on computer vision and pattern recognition*, pages 4700–4708, 2017. 4

[45] Kai Li, Zhengming Ding, Kunpeng Li, Yulun Zhang, and Yun Fu. Support neighbor loss for person re-identification. In *2018 ACM Multimedia Conference on Multimedia Conference*, pages 1492–1500. ACM, 2018. 4, 6

[46] Mingyong Zeng, Chang Tian, and Zemin Wu. Person re-identification with hierarchical deep learning feature and efficient xqda metric. In *2018 ACM Multimedia Conference on Multimedia Conference*, pages 1838–1846. ACM, 2018. 4, 6

[47] Guanshuo Wang, Yufeng Yuan, Xiong Chen, Jiwei Li, and Xi Zhou. Learning discriminative features with multiple granularities for person re-identification. In *2018 ACM Multimedia Conference on Multimedia Conference*, pages 274–282. ACM, 2018. 4, 6, 7

[48] Jiwei Yang, Xu Shen, Xinmei Tian, Houqiang Li, Jianqiang Huang, and Xian-Sheng Hua. Local convolutional neural networks for person re-identification. In *2018 ACM Multimedia Conference on Multimedia Conference*, pages 1074–1082. ACM, 2018. 4, 6, 7

[49] Chunfeng Song, Yan Huang, Wanli Ouyang, and Liang Wang. Mask-guided contrastive attention model for person re-identification. In *Proceedings of the IEEE Conference on Computer Vision and Pattern Recognition*, pages 1179–1188, 2018. 4, 6

[50] Wei Li, Xiatian Zhu, and Shaogang Gong. Harmonious attention network for person re-identification. *2018 IEEE/CVF Conference on Computer Vision and Pattern Recognition*, Jun 2018. 4, 6, 7

[51] Jiawei Liu, Zheng-Jun Zha, Hongtao Xie, Zhiwei Xiong, and Yongdong Zhang. Ca3net. *2018 ACM Multimedia Conference on Multimedia Conference - MM 18*, 2018. 4, 6, 7

[52] Zhun Zhong, Liang Zheng, Guoliang Kang, Shaozi Li, and Yi Yang. Random erasing data augmentation. *arXiv preprint arXiv:1708.04896*, 2017. 5, 6, 7

[53] Mengyue Geng, Yaowei Wang, Tao Xiang, and Yonghong Tian. Deep transfer learning for person re-identification. *arXiv preprint arXiv:1611.05244*, 2016. 5

[54] Liang Zheng, Liyue Shen, Lu Tian, Shengjin Wang, Jingdong Wang, and Qi Tian. Scalable person re-identification: A benchmark. In *Computer Vision, IEEE International Conference on*, 2015. 6, 7

[55] Zhun Zhong, Liang Zheng, Donglin Cao, and Shaozi Li. Re-ranking person re-identification with k-reciprocal encoding. In *Proceedings of the IEEE Conference on Computer Vision and Pattern Recognition*, pages 1318–1327, 2017. 6

[56] Song Bai, Xiang Bai, and Qi Tian. Scalable person re-identification on supervised smoothed manifold. In *Proceedings of the IEEE Conference on Computer Vision and Pattern Recognition*, pages 2530–2539, 2017. 6

[57] Ergys Ristani and Carlo Tomasi. Features for multi-target multi-camera tracking and re-identification. In *Proceedings of the IEEE Conference on Computer Vision and Pattern Recognition*, pages 6036–6046, 2018. 6, 7

[58] Lingxiao He, Jian Liang, Haiqing Li, and Zhenan Sun. Deep spatial feature reconstruction for partial person re-identification: Alignment-free approach. In *Proceedings of the IEEE Conference on Computer Vision and Pattern Recognition*, pages 7073–7082, 2018. 6

[59] Xiaobin Chang, Timothy M Hospedales, and Tao Xiang. Multi-level factorisation net for person re-identification. In *Proceedings of the IEEE Conference on Computer Vision and Pattern Recognition*, pages 2109–2118, 2018. 6, 7

[60] Dapeng Chen, Dan Xu, Hongsheng Li, Nicu Sebe, and Xiaogang Wang. Group consistent similarity learning via deep crf for person re-identification. In *Proceedings of the IEEE Conference on Computer Vision and Pattern Recognition*, pages 8649–8658, 2018. 6

[61] Yantao Shen, Tong Xiao, Hongsheng Li, Shuai Yi, and Xiaogang Wang. End-to-end deep kronecker-product matching for person re-identification. In *Proceedings of the IEEE Conference on Computer Vision and Pattern Recognition*, pages 6886–6895, 2018. 6

[62] Rui Yu, Zhiyong Dou, Song Bai, Zhaoxiang Zhang, Yongchao Xu, and Xiang Bai. Hard-aware point-to-set deep metric for person re-identification. In *Proceedings of the European Conference on Computer Vision (ECCV)*, pages 188–204, 2018. 6

[63] Yantao Shen, Hongsheng Li, Shuai Yi, Dapeng Chen, and Xiaogang Wang. Person re-identification with deep similarity-guided graph neural network. In *Proceedings of the European Conference on Computer Vision (ECCV)*, pages 486–504, 2018. 6

[64] Yifan Sun, Liang Zheng, Yi Yang, Qi Tian, and Shengjin Wang. Beyond part models: Person retrieval with refined part pooling (and a strong convolutional baseline). In *Proceedings of the European Conference on Computer Vision (ECCV)*, pages 480–496, 2018. 6, 7

[65] Cheng Wang, Qian Zhang, Chang Huang, Wenyu Liu, and Xinggang Wang. Mancs: A multi-task attentional network with curriculum sampling for person re-identification. In *Proceedings of the European Conference on Computer Vision (ECCV)*, pages 365–381, 2018. 6, 7

[66] Kai Han, Jianyuan Guo, Chao Zhang, and Mingjian Zhu. Attribute-aware attention model for fine-grained representation learning. In *2018 ACM Multimedia Conference on Multimedia Conference*, pages 2040–2048. ACM, 2018. 6

[67] Mahdi M Kalayeh, Emrah Basaran, Muhittin Gökmen, Mustafa E Kamasak, and Mubarak Shah. Human semantic parsing for person re-identification. In *Proceedings of the IEEE Conference on Computer Vision and Pattern Recognition*, pages 1062–1071, 2018. 6, 7

[68] Jianlou Si, Honggang Zhang, Chun-Guang Li, Jason Kuen, Xiangfei Kong, Alex C. Kot, and Gang Wang. Dual attention matching network for context-aware feature sequence based person re-identification. *2018 IEEE/CVF Conference on Computer Vision and Pattern Recognition*, Jun 2018. 6, 7

[69] Guodong Ding, Salman Khan, Zhenmin Tang, and Fatih Porikli. Let features decide for themselves: Feature mask network for person re-identification, 2017. 7

[70] Zhedong Zheng, Liang Zheng, and Yi Yang. Pedestrian alignment network for large-scale person re-identification, 2017. 7

[71] Xiang Bai, Mingkun Yang, Tengteng Huang, Zhiyong Dou, Rui Yu, and Yongchao Xu. Deep-person: Learning discriminative deep features for person re-identification, 2017. 7

[72] Jon Almazan, Bojana Gajic, Naila Murray, and Diane Larlus. Re-id done right: towards good practices for person re-identification, 2018. 7

[73] Ramprasaath R. Selvaraju, Michael Cogswell, Abhishek Das, Ramakrishna Vedantam, Devi Parikh, and Dhruv Batra. Grad-cam: Visual explanations from deep networks via gradient-based localization. *2017 IEEE International Conference on Computer Vision (ICCV)*, Oct 2017. 7